

Remotely sensed agricultural grassland productivity responses to land use and hydro-climatic drivers under extreme drought and rainfall

Jarrold Kath^{a,*}, Andrew F. Le Brocq^{b,c}, Kathryn Reardon-Smith^a, Armando Apan^{a,b}

^a Centre for Applied Climate Sciences, University of Southern Queensland, Toowoomba, Queensland, 4350, Australia

^b Faculty of Health, Engineering and Sciences, University of Southern Queensland, Toowoomba, Queensland, 4350, Australia

^c Centre for Sustainable Agricultural Systems, University of Southern Queensland, Toowoomba, Queensland, 4350, Australia

ARTICLE INFO

Keywords:

Extreme weather
Millennium drought
Resilience
Pasture
Remote sensing

ABSTRACT

Climate change is expected to increase the frequency and intensity of drought globally with potentially significant consequences for grasslands. We examined grassland responses to a long-term drought on the Darling Downs, eastern Australia, using the Enhanced Vegetation Index (EVI), a remotely sensed measure of primary productivity. This extreme drought period had rainfall deficits comparable to the hottest and driest projected climate change scenarios for 2030 and was followed by extreme rainfall. This juxtaposition allowed investigation of grassland dynamics (decline and recovery) under extreme climatic variability. Our aim was to determine whether factors associated with grassland decline during extreme drought are the same as those that drive recovery post drought. There is limited knowledge about whether the determinants of grassland decline and recovery are consistent, but this information is important for understanding how best to reduce grassland decline, without inhibiting recovery. We calculated EVI (Enhanced Vegetation Index) trends at 2549 grassland sites situated in an agricultural landscape and used boosted regression trees to model these against multiple hydro-climatic and land use factors. As anticipated, hydro-climatic variables were key drivers of EVI trends in both the drought and wet phases, with higher soil moisture corresponding to less decline in the drought phase and enhanced recovery in the wet phase; however, land use and plant trait variables were also important predictors of EVI trends. Higher proportions of dryland agriculture in the local landscape, high C3:C4 ratios and lower proportions of woody vegetation in the local landscape were associated with negative EVI trends (i.e. greater decline) during drought, but had inverse or negligible effects during the post drought recovery phase. Our results suggest that mitigating decline and fostering grassland recovery following drought requires considering multiple hydro-climatic, land use and plant trait drivers and how their importance changes under drought and wet phases.

1. Introduction

A warming world is expected to increase climate variability, including the duration and severity of drought (e.g. Dai, 2013; Trenberth et al., 2013). In dry (e.g. semi-arid) areas, increased drought intensity and frequency under climate change may result in severe vegetation decline and soil degradation, impacting grassland production, reducing the extent of productive pastoral areas and causing widespread economic losses (Tubiello et al., 2007). Increases in the intensity and frequency of droughts could also exacerbate the rate of biodiversity decline (e.g. Choat et al., 2012) and alter ecosystem function (Smith, 2011) globally. Despite these possible socio-economic and ecological implications, drought impacts on grasslands under climate change are

poorly understood, particularly at large scales (e.g. across entire catchments) (Tubiello et al., 2007). An increased understanding of the drivers of grassland decline during drought and recovery after drought is important for determining the longer-term effects of, and hence the resilience of grasslands to, extreme climate variability predicted under climate change.

A number of studies have examined drought responses in grasslands subject to extreme hydro-climatic variability (e.g. D'Odorico and Bhattachan, 2012; Neuwirth and Hofer, 2013; Do and Kang, 2014). However, additional to hydro-climatic effects, land use conditions may also have important effects on grasslands during drought (Oliver and Morecroft, 2014). For ecosystems more generally, there is also recognition that multiple environmental drivers should be considered

* Corresponding author at: Institute for Life Sciences and the Environment, University of Southern Queensland, Toowoomba, West Street, Queensland, 4350, Australia.

E-mail address: kath.jarrod@gmail.com (J. Kath).

<https://doi.org/10.1016/j.agrformet.2019.01.007>

Received 5 October 2018; Received in revised form 27 November 2018; Accepted 4 January 2019

Available online 09 January 2019

0168-1923/ © 2019 Elsevier B.V. All rights reserved.

when investigating drought responses in natural systems (e.g. Dai et al., 2015). Increased warming coupled with reduced rainfall is likely to exacerbate declines in grassland growth rates (Cunha and Richter, 2014), while surrounding land uses, which influence local microclimatic temperatures (Bright et al., 2017) could also have important interactive implications for grassland drought responses. Despite this, studies comparing the influence of multiple drivers on decline and recovery across landscapes are lacking for many environments (but see Gazol et al., 2017).

Drought and other unfavourable climatic conditions can also persist for many years (e.g. parts of the world impacted by the El Niño Southern Oscillation (ENSO)) and their effects can have ongoing consequences for several seasons or years after they occur. For example, Cunha and Richter (2014) suggest climatic variability can impact grassland growth rates in the northeast of Portugal for several years, possibly due to the impacts of temperature on soil organic matter. The impacts of droughts and post-drought recovery on grasslands therefore need to be investigated over multiple years or seasons, particularly in parts of the world influenced by multi-year ENSO phases (e.g. Australia, south Asia, northern South America, the Sahel and southern Africa; Dai, 2013).

Understanding the dynamics of decline and recovery in grasslands is fundamental to modelling the impacts of predicted changes in drought frequency and intensity under climate change (Donohue et al., 2016) and for prioritising and managing the potential trade-offs between actions to reduce decline (e.g. destocking) versus those to increase recovery (e.g. delayed restocking) (Nimmo et al., 2015). Grime et al. (2008) concluded that changing land use and overexploitation rather than climate change were greater threats to fragile grassland ecosystems in northern England. In contrast, Gu et al. (2007) showed strong links between hydro-climatic variables and grassland decline during drought in the central Great Plains, USA, suggesting high sensitivity of these grasslands to climatic change. The importance of drivers of grassland responses to drought may also differ. Some drivers may be key for understanding decline during drought, while others will be more important during recovery post drought (Nimmo et al., 2015). We are unaware of studies which have explicitly tested this in grasslands (although Gazol et al., 2017, investigated this for forests).

We investigated grassland responses (decline and recovery) to drought on the Darling Downs, eastern Australia, using a long-term (2002–2011) remotely sensed dataset. We examined hydro-climatic (e.g. soil moisture and evaporation) and land use (e.g. proportion of woody vegetation and agriculture in the landscape) variables likely to be key drivers of grassland decline and recovery (De Vries et al., 2012; Hoover et al., 2014; De Keersmaecker et al., 2016). Semi-natural grasslands are a widespread and important ecosystem type globally and are an ideal ecosystem for investigating drought because of their relatively high sensitivity to climatic variation (Lindborg et al., 2008) and rapid responses to climatic changes (e.g. Craine et al., 2013). Recent advances in remote sensing technology also allow *in-situ* measurement of long-term and wide-spread continuous change in grassland productivity, which can be mapped and integrated with data on drivers of change (Bright et al., 2017). The remote sensing, hydro-climatic and land use datasets we use in the study are widely available and so the approach we outline could be applied to grasslands globally.

The long-term drought we investigated had rainfall deficits of -8% (relative to a 1986–2005 baseline), comparable to the hottest and driest scenarios of climate change projected for 2030 (CSIRO, 2017). Following the drought, extreme rainfall (ca. + 40% above a 1986–2005 baseline), causing extensive flooding, occurred in 2010–2011 (Bureau of Meteorology (BoM, 2017). This juxtaposition of extreme drought and rainfall provides an opportunity to investigate trends associated with long-term and intense drought and extreme rainfall, both of which are projected to increase under climate change (CSIRO, 2017; Dai, 2013). Specifically, we asked whether key factors associated with grassland decline during an extreme and long-term drought are the same factors

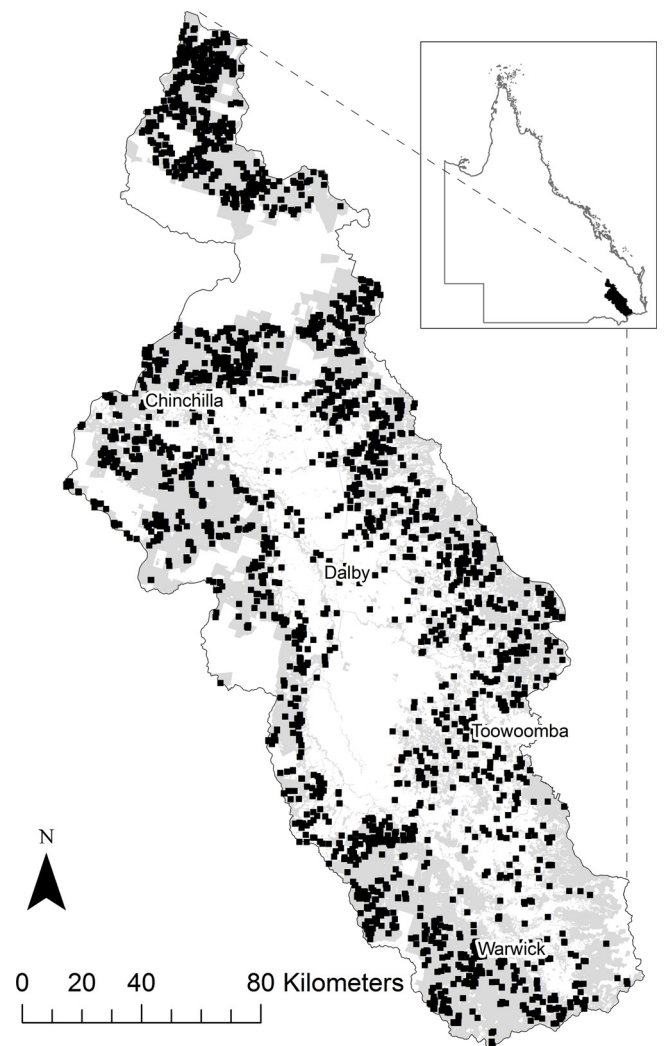


Fig. 1. The study area in southern Queensland, Australia. Grey areas are grazing lands from which enhanced vegetation index time series data from 2549 sites (black squares) were extracted.

that drive grassland recovery post drought following a period of extreme rainfall.

2. Materials and methods

2.1. Study area

The study area covers approximately 30,000 km² on the Darling Downs, eastern Australia (Fig. 1). The area is one of Australia's most agriculturally productive areas (Australian Bureau of Statistics, 2016) with a mix of extensively grazed native grasslands and dryland and irrigated cropping. Average annual rainfall ranges from 673 mm in the west (Chinchilla) to 952 mm in the east (Toowoomba) (Bureau of Meteorology 2017). Recent rainfall variability in the region has been high, with a series of protracted droughts interspersed with intense rainfall events (Bureau of Meteorology 2017) (Fig. 2).

2.2. Study period

Rainfall anomalies were used to classify a long-term (multi-year) drought (May 2002–May 2007) and wetting (May 2006–May 2011) phase. The wet phase included the end of the drought period to ensure that any trend identified was relative to drought conditions (i.e. we wanted to identify the rate of change (trend) in grassland condition

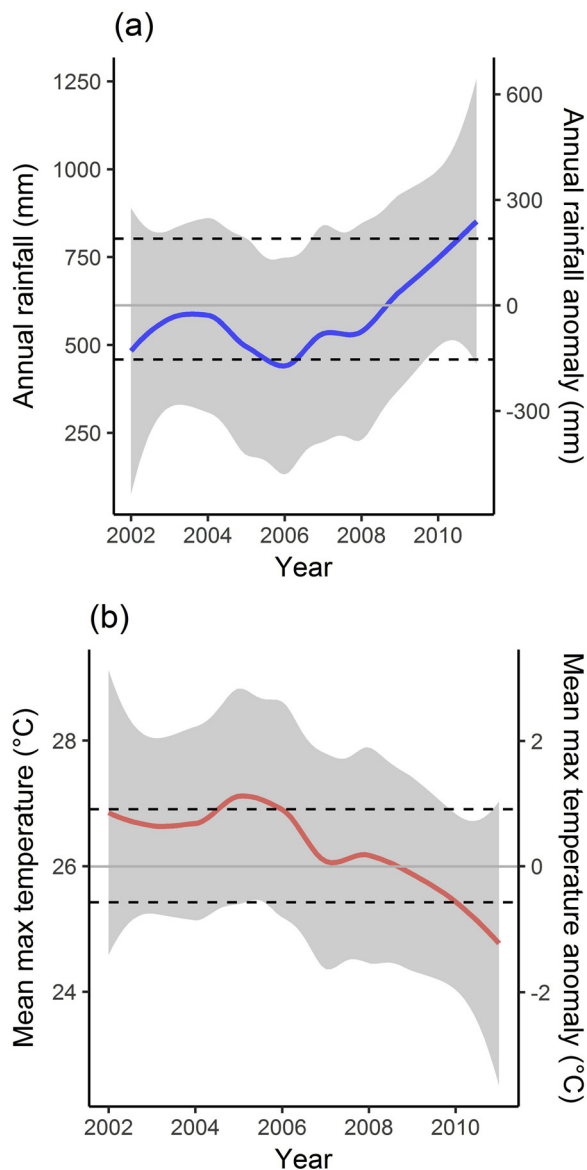


Fig. 2. (a) Average annual rainfall and anomaly (fitted line); and, (b) Average annual maximum temperatures and anomaly relative to the long-term (1986–2005) climatological mean (fitted line) (after CSIRO and Bureau of Meteorology 2017) over the duration of the study. Shaded areas are 95% confidence intervals. Horizontal dashed lines are 10th and 90th percentiles.

emerging from drought and into wetter conditions) so we could assess recovery following dry conditions. The season at the commencement and end of phases and the duration of phases were the same, to avoid any possible biases (Craine et al., 2012). The drought phase included extreme drought conditions (less than the 10th percentile of the long-term 1986–2005 average), while the wet phase included periods of extreme rainfall (greater than 90th percentile of the long-term 1986–2005 average) (after Hundedha and Bárdossy, 2005) (Fig. 2). On average, the drought phase had 160 mm less rainfall per annum and was 1 °C warmer than the wet phase. These two broad climatic periods thus provide an opportunity to examine the long-term before and after effects of protracted drought on these grasslands.

2.3. Enhanced vegetation index (EVI)

Satellite imagery (MODIS and Landsat) provides indicators for many environmental and biotic variables, including vegetation (Pettorelli

et al., 2005). The enhanced vegetation index (EVI) (a newer and bias-corrected version of NDVI) is directly related to the fraction of photosynthetically active radiation. It provides an indicator of primary productivity (Pettorelli et al., 2005) and a robust empirical measure of vegetation activity through time (Eckert et al., 2015). In particular, EVI time-series data has been used to assess and monitor grassland condition and productivity for grazing over extensive areas (e.g. Hua et al., 2017). Higher EVI values indicate greater green biomass and, thus, inferences about changes in grassland green biomass (i.e. primary productivity) can be made. Here we take negative change (trend) in EVI as measure of grassland decline and positive change in EVI as a measure of grassland recovery (after Eckert et al., 2015).

We used EVI data derived from the MODIS Terra sensor using the LPDAAC MOD13Q1 product at nominal 250 m resolution to assess trends in grassland condition (Huete et al., 2002; TERN, 2016a). The MOD13Q1 (16 days maximum value composite EVI) was stacked date sequentially for both the drought and wetting phase over the study period and was filtered for spikes and drops in the data time series. We used the hamper filter from the pracma package (Pearson, 1999; Borchers, 2018) which carries out median deviation computation in the vicinity of each point (following Lyburner et al. (2011), we used a filtering threshold of 2.1 standard deviations) and returns a corrected time series.

We randomly selected 2549 sites (representing ~ 25% of all possible grassland sites) from areas mapped as grasslands (Department of Science, Information Technology and Innovation (DSITI, 2017), which ensured a spread of sites across the study area. Sites with woody vegetation cover were excluded so that responses represented those of homogenous grassland areas (i.e. areas that were mapped as grasslands and had less than 1% cover of woody vegetation). Fig. 3 shows mean EVI values in the drought and wet phase across all selected sites, as well as example time profiles for selected sites across the study period. At each site, EVI values were derived as a time-series of each phase. For EVI, one value (i.e. a value from each scene, which is the area on the ground the measure applies to over the duration of time specified) for every 16 days was aggregated to mean monthly values to facilitate integration with monthly values of hydro-climatic data. At each site, during each climate phase, there were 116 scenes, which were then aggregated to monthly values ($n = 61$ for each phase) for trend analysis.

2.4. EVI trend analysis

Trends in grassland EVI (mean monthly values) at each site were calculated using Mann–Kendall tests (after Kath et al., 2015; Le Brocq et al., 2018). Mann–Kendall is a nonparametric test used to quantify trends in time-series data and commonly used to assess trends in environmental responses (Kendall, 1955; Menzel and Fabian, 1999). The ‘Zhang’ (Zhang et al., 2000) method was used to compute pre-whitened nonlinear trends (i.e. detrended for serial autocorrelation—e.g. seasonality—which could violate the assumptions of analyses, e.g. uncorrelated errors) and conducted using the ZYP (Bronaugh and Werner, 2013) and Kendall (McLeod, 2011) packages in R (R Core Development Team, 2016). Declining EVI was taken as a measure of grassland decline in the drought phase and increasing EVI taken as a measure of grassland recovery in the wet phase—the more negative the trend, the greater the decline and the more positive the trend, the greater the recovery. Trends from the drought and wet phases were used as a response in statistical models to identify key drivers of decline and recovery (after Kath et al., 2015).

2.5. Hydro-climatic and land use data

We used 13 variables representing a range of hydro-climatic and land use factors to model grassland EVI trends in the drought and wet phase (Table 1). Land use factors were: cattle density, which were

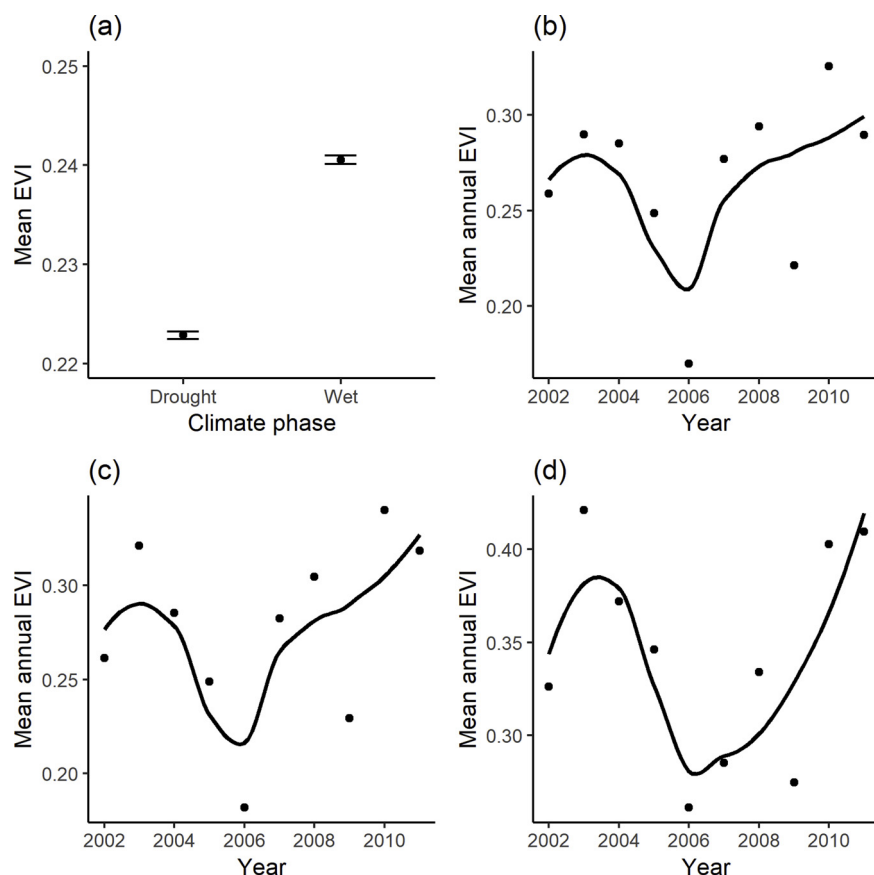


Fig. 3. (a) Mean EVI values in the drought and wet phase across all sites (error bars are 95% confidence intervals), as well as example (b)–(d) time profiles for selected sites across the study period.

Table 1

Predictor variable descriptions, notes on analysis and data sources.

Variable description	Analysis notes and data source
*Potential evapotranspiration (PET) trend (atmospheric demand) (mm)	Calculated using the ‘Zhang’ (Zhang et al., 2000) method for computing pre-whitened nonlinear trends [i.e. de-trended for serial autocorrelation ZYP (Bronaugh and Werner, 2013) and Kendall (McLeod, 2011) packages in R (R Core Development Team, 2016)].
*Potential evapotranspiration (PET) anomaly (atmospheric demand) (mm)	Anomalies were calculated proportional to recent long-term mean site conditions from 2000–2014 (i.e. anomaly/site mean).
*Top soil moisture layer trend (0–10 cm) (mm)	As for trend calculation above
*Top soil layer anomaly (0–10 cm) (mm)	As for anomaly calculation above
*Mid soil moisture layer trend (10–100 cm) (mm)	As for trend calculation above
*Mid soil moisture layer anomaly (10–100 cm) (mm)	As for anomaly calculation above
*Deep soil moisture layer trend (100–500 cm) (mm)	As for trend calculation above
*Deep soil moisture layer anomaly (100–500 cm) (mm)	As for anomaly calculation above
Dryland agriculture - Proportion of dryland agriculture in local drainage area	Land that is used principally for primary production, based on dryland farming systems. Dryland agriculture, irrigated agriculture and woody vegetation cover data were from Queensland government land use mapping (Department of Science, Information Technology and Innovation (DSITI, 2017) which use available databases, satellite imagery and aerial photos to classify land use. Drainage units are from the Australian Bureau of Meteorology, Australian Hydrological Geospatial Fabric (Geofabric) (Commonwealth of Australia, 2015).
Irrigated agriculture - Proportion of irrigated agriculture in local drainage area	Agricultural land uses where water is applied to promote additional growth. See Dryland agriculture above for methods of calculation.
Woody vegetation cover - Proportion of woody vegetation in local drainage area	Areas covered by perennial woody vegetation. See Dryland agriculture above for methods of calculation.
Mean cattle density - Modelled cattle livestock numbers for each site	Food and Agriculture Organisation (FAO) modelled livestock densities, corrected using official (FAOSTAT) national estimates for the reference year 2005, at a spatial resolution of 3 minutes of arc (about 5 × 5 km at the equator) (Robinson et al., 2014).
Ratio of C3 to C4 plants - Calculated for each year and averaged across each dry and wet period for analysis.	From the MODIS Gross Primary Productivity - DIFFUSE algorithm with three-veg-type parameterisation from TERN AusCover (2016b) (http://www.auscover.org.au) and retrieved from the online Data Pool, courtesy of the NASA Land Processes Distributed Active Archive Center (LP DAAC), USGS/Earth Resources Observation and Science (EROS) Center, Sioux Falls, South Dakota, https://lpdaac.usgs.gov/data_access/data_pool .

* Extracted from the Australian Bureau of Meteorology, Australian Water Resources Assessment Landscape model (AWRA-L v5.0) – A modelled daily time series of climatic and soil moisture variables on a 5 km grid (Australia Water Resources Assessment, 2017).

modelled livestock densities corrected using official (FAOSTAT) national estimates for the reference year 2005 (from Robinson et al., 2014); and proportion of dryland agriculture, irrigated agriculture and native woody vegetation in the local drainage area (partitioning of land uses followed the Australian Land Use and Management (ALUM) Classifications system; see Table 1 for details). We also included data on the ratio of C3 to C4 plants (derived using the MODIS Gross Primary Productivity - DIFFUSE algorithm, TERN, 2016b; Table 1) which is known to be an important intrinsic trait influencing grassland response to drought (Hoover et al., 2014). While the C3:C4 ratio is derived from MODIS, it represents a measure of grassland composition (i.e. the relative proportion of grasses that are either C3 or C4) and as such is qualitatively different from the MODIS measure of EVI and from our response variable, EVI trend, which represents the rate of change in total green biomass through time at each site. The simple linear correlation between these two variables is also low (Pearson $r < |0.2|$).

Hydro-climatic variables were: anomalies (relative to the mean for the entire period from May 2002 to May 2011) and trends in soil moisture at top (0–10 cm), mid (10–100 cm) and deep (100–500 cm) soil depths, and potential evapotranspiration (PET) derived from the Australian Water Resources Assessment Landscape model (AWRA-L v5.0; Australia Water Resources Assessment, 2017)—a modelled daily time series of climatic and soil moisture variables (Australia Water Resources Assessment, 2017) (Table 1). Where it has been tested, the AWRA-L model predicts soil moisture with good accuracy (Pearson r of ~ 0.75) (Hafeez et al., 2015; Viney et al., 2015). Soil moisture variables were used instead of rainfall, because they are more proximal drivers of grassland biomass (Polley et al., 2013). We included both trends and anomalies for soil moisture and evaporation variables to assess both rate of change (trend) and magnitude of change (anomaly).

Correlations between all predictors were $|r| < 0.70$, the level at which collinearity can affect regression models (Dormann et al., 2013), except for the topsoil trend moisture variable, which was correlated with midsoil moisture anomaly ($r = 0.75$) and topsoil moisture anomaly ($r = 0.78$) in the drought phase (Appendix A). The relationships between predictor variables in wet and drought phases are shown using principal component analysis in Fig. 4. We ran models without the topsoil trend variable, but this did not alter model results or the importance of variables and so it was retained to allow direct comparison of drought and wet phase models (Appendix B). Summary statistics for predictor variables are given in Appendix D.

2.6. Modelling grassland responses to land use and hydro-climatic drivers

We modelled grassland decline (EVI trends in the drought phase) and recovery (EVI trends in the wet phase) using boosted regression trees (BRTs). BRTs derive from machine learning and are well suited for modelling complex functions without making assumptions about the shape of the fitted functions (Elith et al., 2006). BRTs have several advantages—they efficiently handle different data types and missing data; do not require predictor transformations; and automatically handle interaction effects between predictors (Elith et al., 2006). Analyses were carried out in R (Version 3.3.0; R Development Core Team, 2016) using the 'gbm' library (Ridgeway, 2012) supplemented with functions from Elith et al. (2008). All BRT models were optimised for their learning rate so that a minimum of 1000 trees was fitted (after Elith et al., 2008). The relative contributions of each predictor variable to the BRT models were assessed on the basis of the number of times a predictor was selected for splitting, weighted by the squared improvement to the model as a result of each split, and averaged over all trees (after Elith et al., 2008).

To investigate whether drivers had a similar relationship with grassland decline and recovery, we examined the Pearson correlation between predicted EVI trends during the drought and wet phase for each driver, while controlling for the average effect of other variables in the model (Elith et al., 2008). Positive correlations between predicted EVI trends in the drought and wet phase would indicate similar responses, or congruence, to that driver, while negative correlations would indicate a potential trade-off between decline and recovery in relation to that driver.

Model performance was assessed using cross-validated correlation (CV correlation), which provides a measure of correlation between the recorded observations and the model fitted values and thus the predictive accuracy of the model. CV correlation is calculated as a Pearson correlation coefficient and takes into account how far the prediction varies from the observed data (Parviainen et al., 2009). Validation was performed by 10-fold cross validation (i.e. splitting the data into 10 subsets, with the model being fit on one subset (build) and tested on an independent (testing/holdout set) with the average holdout residual deviance used to identify the optimum number of trees (i.e. when the holdout deviance is minimised) (after Hastie et al., 2001; Elith et al., 2008). Residual spatial autocorrelation, which can bias parameter estimates, was controlled for by using the residual autocovariate (RAC) method (after Crase et al., 2012). The RAC method controls spatial

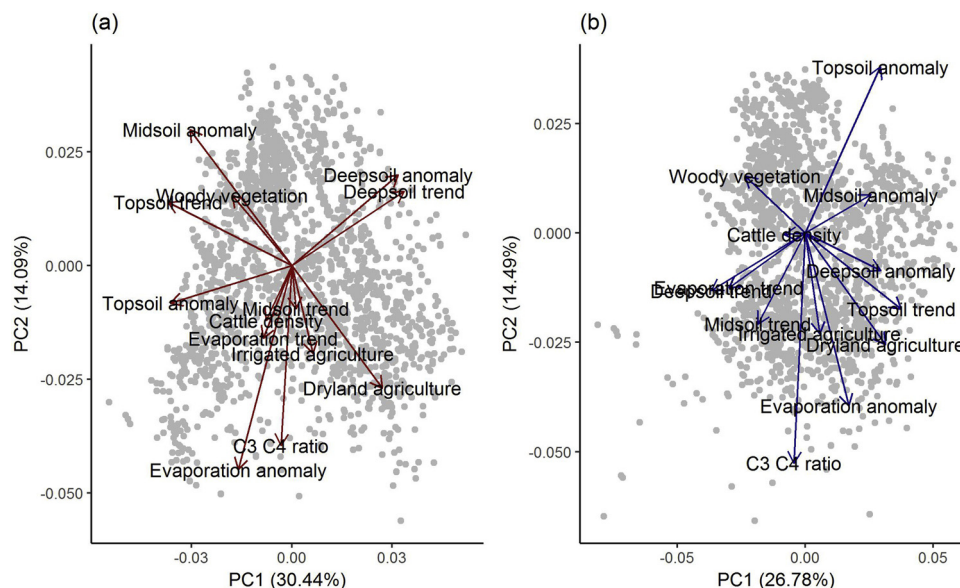


Fig. 4. Principal component analysis showing the relationship between hydro-climatic predictors during the drought and wet phase.

Table 2
Model performance and relative importance of driver for grassland drought and wet phase models assessed by boosted regression trees and summary of relationship to EVI trends exhibited in Figs. 4 and 5 and Appendix C.

	Model performance: Drought		Model performance: Wet Phase	
	Cross validated observed-predicted correlation* (standard error)	0.69 (0.01) 3 550	0.61 (0.01) 2 550	
Number of trees fitted in model				
	Drought Driver BRT relative importance (%)	Effect on EVI trends during drought	Wet Phase Driver BRT relative importance (%)	Effect on EVI trends during wet phase
Deepsoil moisture anomaly	3.78	Weakly reducing	3.95	Weakly enhancing
Deepsoil moisture trend	3.57	Weakly reducing	4.04	Weakly enhancing
Proportion of dryland agriculture	22.92	Intensifying	7.71	Negligible
Evaporation anomaly	4.28	Negligible	10.17	Inhibiting
Evaporation trend	3.90	Negligible	4.93	Negligible
Proportion of irrigated agriculture	2.04	Negligible	1.97	Negligible
Mean cattle density	4.59	Negligible	6.85	Enhancing
Midsoil moisture anomaly	18.53	Reducing	7.12	Enhancing
Midsoil moisture trend	5.76	Reducing	17.88	Enhancing
Ratio of C3 to C4 plants	11.58	Intensifying	12.59	Enhancing
Topsoil moisture anomaly	8.63	Reducing	7.79	Enhancing
Topsoil moisture trend	4.29	Reducing	5.80	Enhancing
Proportion of woody vegetation	6.14	Reducing	9.20	Inhibiting

* CV correlation is calculated as a Pearson r correlation coefficient.

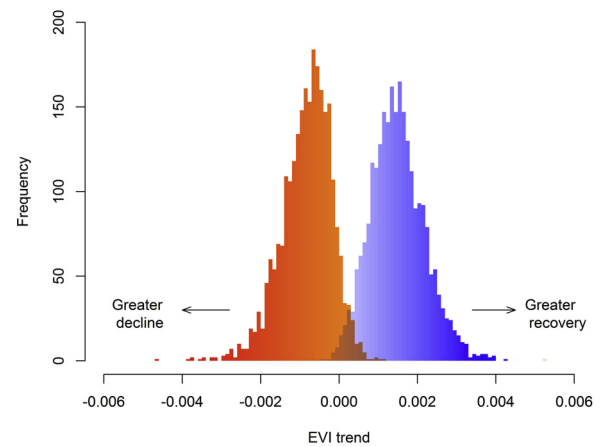


Fig. 5. Histogram of EVI trends in the drought period (left hand side and red) and wet period (right hand side and blue) (For interpretation of the references to colour in this figure legend, the reader is referred to the web version of this article).

autocorrelation by fitting the explanatory environmental variables with an autocovariate representing the residuals in the environmental only model (see Crase et al., 2012).

3. Results

3.1. Model performance and relative importance of drivers of EVI trends

Models of grassland EVI trends in the drought and wet phase performed well: cross validated model performance was 0.69 for drought phase EVI trend model and 0.61 for the wet phase EVI trend model (Table 2). Grassland EVI trends in the drought phase were largely declining (2364 of 2549 sites; Figs. 5 and 6a), while the wet phase EVI trends were mostly increasing (2529 of 2549 sites; Figs. 5 and 6b). Across all sites there was an average ca. 23% decline in EVI during the drought phase, while during the wet phase there was an average ca. 57% increase in EVI.

The proportion of dryland agriculture in the local drainage area was the strongest predictor (22.9% relative importance) of declining EVI for the drought phase, followed by midsoil moisture anomaly (18.5%), ratio of C3:C4 plants (11.6%), and topsoil moisture anomaly (8.6%) (Table 2). Midsoil moisture trend (17.9%), C3:C4 plants (12.6%), evaporation anomaly (10.2%) and proportion of woody vegetation in the local drainage area (9.2%) were the strongest predictors of increasing EVI in the wet phase (Table 2).

3.2. Drivers of grassland decline during drought

During drought, there were negative relationships between declining EVI and proportion of dryland agriculture in the local drainage area and C3:C4 ratio, and positive relationships between declining EVI and midsoil moisture anomaly, proportion of woody vegetation in the local drainage area, topsoil moisture anomaly, and midsoil moisture trend (Fig. 7). Higher proportion of dryland agriculture and C3:C4 ratio and lower topsoil and midsoil moisture anomalies, proportion of woody vegetation in the local drainage area, and midsoil moisture trend were associated with stronger declining EVI (i.e. greater decline) during drought (Fig. 7).

3.3. Drivers of grassland recovery during wet phase

During the wet phase, there were positive relationships between increasing EVI and midsoil moisture trend, topsoil moisture anomaly, C3:C4 ratio, and proportion of dryland agriculture in the local drainage

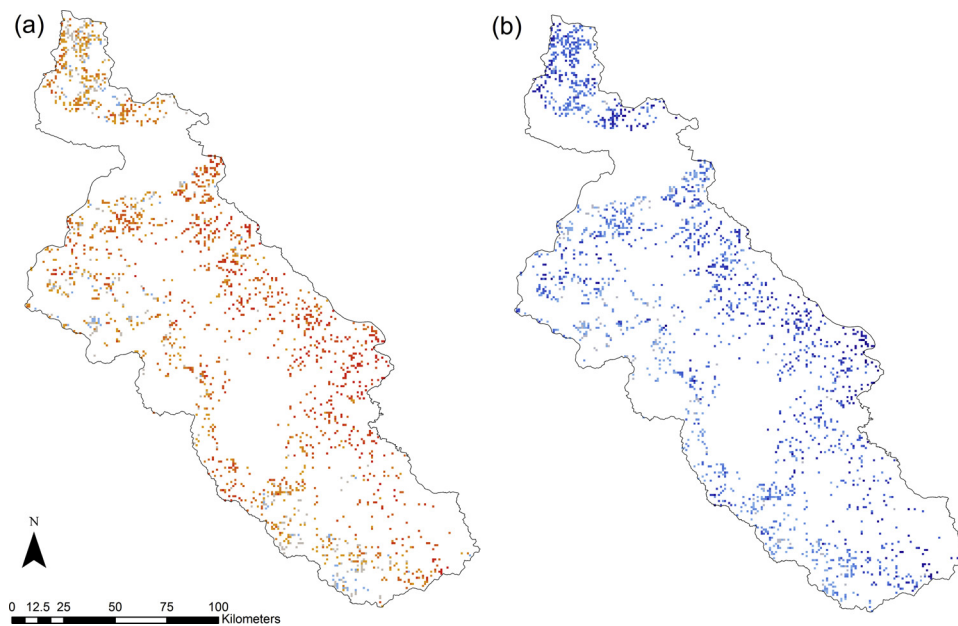


Fig. 6. (a) Mapped EVI trends across study area in the drought period; and, (b) mapped EVI trends across study area in the wet period. Red = negative trends; blue = positive trends. The more intense the colour, the stronger the trend at that site (For interpretation of the references to colour in this figure legend, the reader is referred to the web version of this article).

area, and negative relationships between increasing EVI and evaporation anomaly and proportion of woody vegetation in the local drainage area (Fig. 8). Positive soil moisture anomalies, higher soil moisture trends and C3:C4 ratio, as well as lower evaporation anomalies and proportions of woody vegetation in the local drainage area were associated with stronger increasing EVI (i.e. greater recovery) during the wet phase (Fig. 8).

3.4. Correlations between drivers of EVI trends

All predicted EVI trends for decline and recovery for each driver, except the proportion of irrigated agriculture in the local drainage area, were significantly correlated (Pearson's r correlation, $P < 0.001$; Table 3). Positive correlations indicating similar responses to drivers in drought and wet phases were evident for soil moisture (topsoil, midsoil and deepsoil) anomalies and trends (Table 3). Negative correlations indicating trade-offs between grassland decline and recovery were evident for proportions of dryland agriculture and woody vegetation in the local drainage area, evaporation anomaly and trend, and C3:C4 ratio (Table 3).

4. Discussion

Extreme and long-term drought provides an opportunity to understand the potential future impacts of climate change on grassland dynamics. We modelled enhanced vegetation index (EVI) trends, which represent the fraction of photosynthetically active radiation and provide a measure of grassland primary productivity change, as a function of multiple variables to identify the main drivers of productivity under extreme climate variability and to understand whether the drivers of decline and recovery were concordant. In this study, multiple drivers explained declining grassland EVI during drought and increasing EVI during the subsequent wet phase. While many of the drivers tested influenced both grassland decline and recovery, a number of these had differential effects across the climate phases. Soil moisture drivers were concordant, showing similar relationships by reducing decline in terms of grassland productivity in the drought and enhancing recovery in the wet phase. However, evaporation and land use factors were dissonant, exhibiting either negligible effects or inverse effects between the climatic phases. For example, the proportion of dryland agriculture in the local drainage area was an important predictor of grassland decline for the drought phase, having an intensifying effect on grassland

productivity, but of low relative importance in the wet phase. Potential evapotranspiration (evaporation anomaly) was an important predictor of grassland productivity in the wet phase having a strong inhibiting effect on recovery, but of low relative importance in the drought.

4.1. Possible explanations for different effects of drivers between extreme drought and wet phases

In contrast to hydro-climatic drivers, the land use drivers (proportions of dryland agriculture and woody vegetation in local drainage area), as well as the plant trait factor C3:C4 ratio, had different effects on grassland productivity in the drought and wet phases. Somewhat counter-intuitive is the observation here that the proportion of dryland agriculture has an intensifying effect on grassland productivity in drought, but little effect on recovery during the wet phase, whereas the proportion of woody vegetation in local drainage area reduced decline in drought, but had an inhibiting effect on recovery. De Keersmaecker et al. (2016) showed that semi-natural grasslands underwent less decline than agricultural grasslands in response to climate anomalies, but also that they had lower rates of recovery. While it is not unreasonable to expect higher agriculture and lower woody vegetation cover in the landscape would increase local microclimatic temperatures (Bright et al., 2017), thereby exacerbating drought impacts on grasslands, the negligible effect of agriculture and inhibiting effect of woody vegetation on grassland recovery are more difficult to explain. It is possible that during the wet phase, the microclimatic influences of dryland agriculture become less important, while higher woody vegetation in local drainage area may inhibit grassland recovery through competition for moisture between neighbouring forest/woodland and grassland species (de Dios et al., 2014). In a fine scale experiment, Moreno (2008) also highlighted that trees can have both negative and positive effects on grassland biomass, possibly by competing for soil water and through shading, respectively.

Unlike the soil moisture variables, evaporation anomalies showed a different relationship with degradation and recovery. During the drought phase, evaporation anomalies had no discernible relationship with EVI trends. In contrast, during the wet phase, higher evaporation anomalies were strongly related to EVI trends, with evaporation being associated to lower recovery. Hoover et al. (2014) also found no effects of heat treatments (similar to our measure of evaporation) on grassland above ground net primary productivity under drought. We are unaware of any landscape scale studies that have tested heat or evaporation

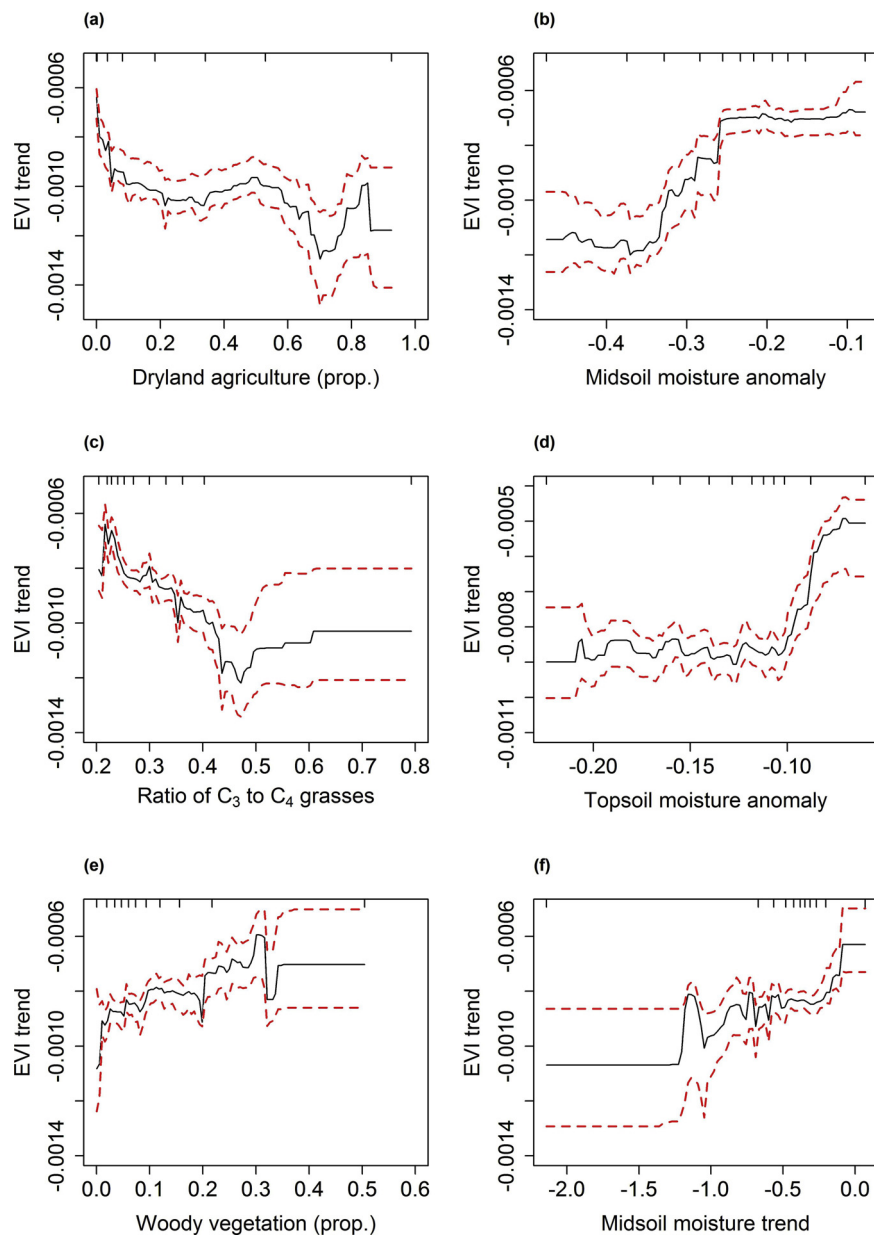


Fig. 7. Relationship of main drivers of grassland EVI trend response during drought: (a) proportion of dryland agriculture; (b) midsoil moisture anomaly; (c) C3:C4 ratio; (d) topsoil moisture anomaly; (e) proportion of woody vegetation; and, (f) midsoil moisture trend. Dashed lines are 95% confidence intervals (representing the precision of predictions).

impacts on grasslands under extreme wet periods following drought. One potential explanation for our results is that, in the drought phase, soil moisture is the chief limiting factor on grassland productivity while, in the wet phase, soil moisture is no longer limited and so growth then becomes limited by evaporation. Further, experimental work is needed to test this mechanism.

These results, while broadly consistent with other studies (Hoover et al., 2014; Hofer et al., 2016), also show that the importance of drivers can vary depending on climatic conditions. Grime et al. (2008) concluded that changing land use and overexploitation, rather than climate change *per se* are the key drivers of change in grasslands they examined in northern England. Our results support this assertion under drought conditions for southern Queensland grasslands, but we also show that this may not be the case during grassland recovery accompanying wet phases. Likewise, experimental studies on grasslands demonstrate the importance of soil moisture and traits as drivers of both decline and recovery (Hoover et al., 2014; Hofer et al., 2016), but are

often unable to examine broader land use effects (e.g. agricultural and woody vegetation cover) as we have in this study.

Hydro-climatic variables (soil moisture, temperature, evapotranspiration) are widely recognised as key drivers of grassland productivity (e.g. Polley et al., 2013). Not surprisingly in this study, lower soil moisture availability corresponded to greater grassland decline, while higher soil moisture availability increased recovery. Other studies show that soil moisture—or its ultimate driver, precipitation—is strongly related to grassland biomass change (i.e. decline and recovery) (Hoover et al., 2014; Hofer et al., 2016). In general, grasslands are expected to benefit under predicted climate warming and the increased frequency and intensity of extreme climate events (Grime et al., 2008; Godfree et al., 2011; Craine et al., 2013). High species diversity and the physiological drought-tolerance of many species found in semi-natural grasslands are expected to facilitate resilient grassland ecosystems under climate change (Craine et al., 2013).

One possible mechanism for this is evident in the current study in

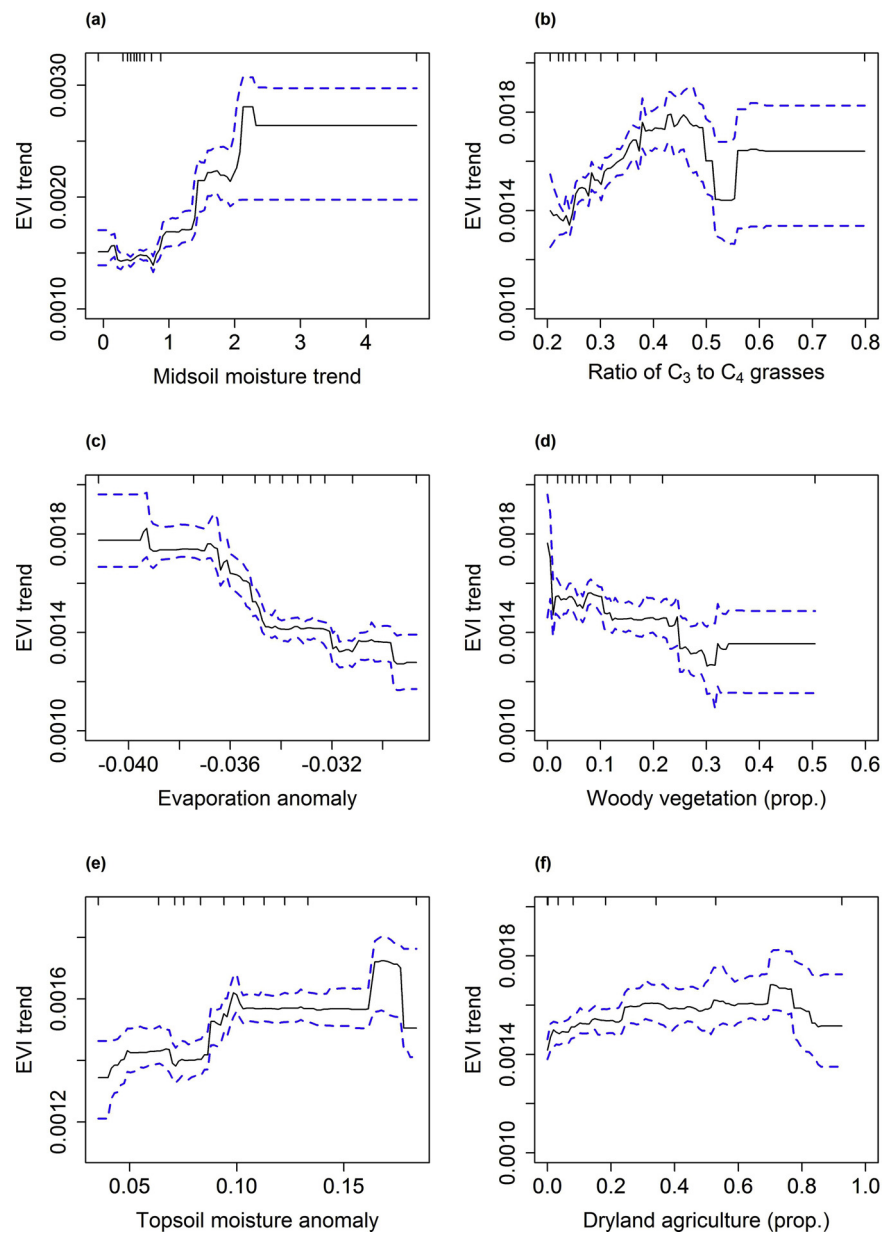


Fig. 8. Relationship of main drivers of grassland EVI trend response during wet phase: (a) midsoil moisture trend; (b) C3:C4 ratio; (c) evaporation anomaly; (d) proportion of woody vegetation; (e) topsoil moisture anomaly; and, (f) proportion of dryland agriculture. Dashed lines are 95% confidence intervals (representing the precision of predictions).

Table 3

Pearson's r correlations between predicted hydro-climatic and land use drivers of grassland responses during drought and wet phases. Positive correlations between drought and wet phases indicate similar responses or congruence to that driver. Negative correlations indicate a potential trade-off between decline and recovery in relation to that driver.

Driver	Pearson's r correlation	p-value	95% CI lower bound	95% CI upper bound	t-value
Deepsoil moisture anomaly	0.62	< 0.001	0.58	0.66	25.24
Deepsoil moisture trend	0.30	< 0.001	0.24	0.36	9.95
Proportion of dryland agriculture	-0.59	< 0.001	-0.63	-0.55	-22.99
Evaporation anomaly	-0.49	< 0.001	-0.53	-0.44	-17.72
Evaporation trend	-0.61	< 0.001	-0.65	-0.57	-24.59
Proportion of irrigated agriculture	0.05	0.09	-0.01	0.12	1.69
Mean cattle density	-0.30	< 0.001	-0.35	-0.24	-9.76
Midsoil moisture anomaly	0.76	< 0.001	0.73	0.79	37.10
Midsoil moisture trend	0.78	< 0.001	0.76	0.81	39.96
Ratio of C3 to C4 plants	-0.63	< 0.001	-0.67	-0.60	-25.88
Topsoil moisture anomaly	0.57	< 0.001	0.52	0.61	21.66
Topsoil moisture trend	0.65	< 0.001	0.61	0.68	26.85
Proportion of woody vegetation	-0.87	< 0.001	-0.89	-0.86	-57.08

the strong predictive response of the ratio of C3:C4 plants in the drought and wet phase models. Sites with lower C3:C4 ratios (i.e. a higher proportion of C4 plants) underwent less decline, although higher C3:C4 ratios (i.e. a higher proportion of C3 plants) enhanced recovery. Hoover et al. (2014) also noted increased sensitivity of C3 vegetation to experimental droughts compared to that of C4 grasses. The advantage of C4 metabolism in maintaining higher water use efficiencies under drier conditions (Luo et al., 2018) imparts a degree of resistance in the drying phase of the climate cycle. One possible problem for grasslands might be that the changing drought/wet regime might select for C4 grasses over longer timescales; while conferring higher resistance to drought, this may reduce the ability of the grassland ecosystem to recover once water use efficiencies are less limiting. Longer-term research on the species compositional and functional changes in semi-natural grasslands under extreme climate events is required to explore this possible mechanism. Regardless of underlying mechanisms, our study shows grassland productivity, as determined by EVI, is highly responsive to extreme climate variability through the measured hydro-climatic drivers; however, these are not the only drivers of trends in grassland productivity.

Other factors not examined here may also be important drivers of grassland decline and recovery to drought. For example, nitrogen fertilisation is reported to facilitate grassland recovery (Carlsson et al., 2017). Grazing is also known to be an important driver of grassland decline; while we included grazing in our model, the best available data was at the broad 5 x 5 km scale, whereas grazing impacts may be better understood at finer scales (Deléglise et al., 2015, but see Kawamura et al., 2005 who suggested grazing can be monitored at broad scales using remote sensing technologies). Nonetheless, our models explained high levels of the variation in grassland productivity to drought and we accounted for residual spatial correlation in our models, so these limitations do not place in question our findings regarding the role of the hydro-climatic and land use drivers examined in this study.

The time and spatial scales examined in this study should also be considered when interpreting our results. In this study, we were focused on making generalisations about longer term and larger scale grassland response and recovery to extended periods of extreme drought and wetting phases and so looked at responses at the entire catchment scale over multiple years. Future research, using a similar approach used here, could investigate finer, or different, spatial and temporal scale grassland dynamics under extreme drought and rainfall conditions. For example, using daily climatic data and investigating shorter term responses, one could examine the impacts of grasslands to extreme events occurring over a few months (e.g. ‘flash droughts’; Otkin et al., 2016) or a single season *in-situ* as has been done in experimental studies (e.g. seasonal rainfall reductions of ~ 66%; Hoover et al., 2014). Similarly, examining grassland responses within a particular landscape type or climatic zone would enable the generality of our findings to be tested. Grassland responses to extreme drought and wet phases may differ markedly in arid grazing dominated landscapes compared to the mixed agriculture sub-tropical/temperate landscape we investigated. Our analytical approach takes into account interactions between the hydro-climatic and land use predictors examined (Elith et al., 2008), as well as accounting for spatial autocorrelation (Crase et al., 2012); thus, our analysis is not biased by the range of conditions under which grassland responses were examined. It is nonetheless important to keep in mind that analysis carried out over different scales could yield different insights into how grasslands respond to extreme climatic conditions.

4.2. Implications for managing grassland responses to drought

The dissonant results for agricultural land cover, woody vegetation cover and the ratio of C3 to C4 plants observed here suggest there are trade-offs (*sensu* Nimmo et al., 2015) in the role of these factors that, if dynamically managed, may reduce the extent of grassland decline under drought and maximise recovery following drought. For example,

reducing the intensity of dryland agriculture and increasing woody vegetation cover through revegetation in areas adjacent to grasslands could decrease the rate of productivity decline during long-term droughts. Similarly, increasing the proportion of C4 plants in grasslands could help minimise decline under drought. Conversely, actions such as reducing woody vegetation cover, for example through thinning (Hall et al., 2016), and managing grasslands to ensure retention of C3 species could enable more rapid grassland recovery following drought.

4.3. Conclusions

Our study has three key findings. First, the relative importance of predictors differed between grassland decline and recovery phases. Second, land use and plant trait drivers, as well as hydro-climatic drivers, are important predictors of grassland productivity. Third, grassland decline and recovery trends were congruent for hydro-climatic variables, but not for the land use factors or the trait factor, ratio of C3 to C4 plants. These findings will contribute to increased understanding of the effects of climate variability, and extreme climate events in particular, on decline and recovery processes (i.e. resilience to climate variability) in agriculturally important semi-natural grasslands.

Acknowledgements

This study was partly supported by the Queensland Drought Mitigation Centre under the Drought and Climate Adaptation Program (DCAP). The authors also thank the Centre for Applied Climate Sciences (ICACS) at the University of Southern Queensland for logistic support.

Appendix A. Supplementary data

Supplementary material related to this article can be found, in the online version, at doi:<https://doi.org/10.1016/j.agrformet.2019.01.007>.

References

- Australia Water Resources Assessment, 2017. Australian Bureau of Meteorology, Australian Water Resources Assessment Landscape Model (AWRA-L v5.0). Accessed 20 August 2016. http://www.bom.gov.au/water/landscape/#/sm_pct/Actual/Day/-39.00/130.40/4/Point/Separate//2017/8/31.
- Australian Bureau of Statistics, 2016. Value of Agricultural Commodities Produced, Australia, 2014–15. Available from. Australian Bureau of Statistics, Canberra Accessed 17 April 2017. <http://www.abs.gov.au/AUSSTATS/abs@.nsf/DetailsPage/7503.02014-15?OpenDocument>.
- Borchers, H.W., 2018. Pragma: Practical Numerical Math Functions. R Package Version 2.1.5. <https://CRAN.R-project.org/package=pragma>.
- Bright, R.M., Davin, E., O'Halloran, T., Pongratz, J., Zhao, K., Cescatti, A., 2017. Local temperature response to land cover and management change driven by non-radiative processes. *Nat. Clim. Chang.* 7, 296–302. <https://doi.org/10.1038/nclimate3250>.
- Bronaugh, D., Werner, A., 2013. Zyp: Zhang + Yue-Pilon Trends Package. R Package Version 0.10-1. <http://CRAN.R-project.org/package=zyp>.
- Bureau of Meteorology (BoM), 2017. Climate Data Online. Available at: Australian Government Bureau of Meteorology (BoM), Melbourne, Vic., Australia Accessed 29 August 2016. <http://www.bom.gov.au/climate/data/>.
- Carlsson, M., Merten, M., Kayser, M., Isselstein, J., Wrage-Mönnig, N., 2017. Drought stress resistance and resilience of permanent grasslands are shaped by functional group composition and N fertilization. *Agric. Ecosyst. Environ.* 236, 52–60. <https://doi.org/10.1016/j.agee.2016.11.009>.
- Choat, B., Jansen, S., Brodribb, T.J., Cochard, H., Delzon, S., Bhaskar, R., Bucci, S.J., Field, T.S., Gleason, S.M., Hacke, U.G., Jacobsen, A.L., Lens, F., Maherali, H., Martínez-Vilalta, J., Mayr, S., Mencuccini, M., Mitchell, P.J., Nardini, A., Pittermann, J., Pratt, R.B., Sperry, J.S., Westoby, M., Wright, I.J., Zanne, A.E., 2012. Global convergence in the vulnerability of forests to drought. *Nature* 491, 752–755. <https://doi.org/10.1038/nature11688>.
- Commonwealth of Australia, 2015. Australian Hydrological Geospatial Fabric (Geofabric). the Bureau of Meteorology 2015 Accessed 23 September 2016. <ftp://ftp.bom.gov.au/anon/home/geofabric/>.
- Craine, J.M., Nippert, J.B., Elmore, A.J., Skibbe, A.M., Hutchinson, S.L., Brunsell, N.A., 2012. Timing of climate variability and grassland productivity. *Proc. Natl. Acad. Sci.* 109, 3401–3405. <https://doi.org/10.1073/pnas.1118438109>.
- Craine, J.M., Ocheltree, T.W., Nippert, J.B., Towne, E.G., Skibbe, A.M., Kembel, S.W., Fargione, J.E., 2013. Global diversity of drought tolerance and grassland climate-change resilience. *Nat. Clim. Chang.* 3, 63.

- Crane, B., Liedloff, A.C., Wintle, B.A., 2012. A new method for dealing with residual spatial autocorrelation in species distribution models. *Ecography* 35, 879–888.
- CSIRO, 2017. Climate Change in Australia. Projections for Australia's NRM Regions. Accessed 04/07/2017. <https://www.climatechangeinaustralia.gov.au/en/climate-projections/climate-analogues/analogues-explorer/>.
- Cunha, M., Richter, C., 2014. A time-frequency analysis on the impact of climate variability with focus on semi-natural montane grassland meadows. *IEEE Trans. Geosci. Remote Sens. (TGRS)* 52 (10), 6156–6164.
- D'Odorico, P., Bhattachan, A., 2012. Hydrologic variability in dryland regions: impacts on ecosystem dynamics and food security. *Philos. Trans. Biol. Sci.* 367, 3145–3673157. <https://doi.org/10.1098/rstb.2012.0016>.
- Dai, A., 2013. Increasing drought under global warming in observations and models. *Nat. Clim. Chang.* 3, 52–58. <https://doi.org/10.1038/nclimate1633>.
- Dai, L., Korolev, K.S., Gorea, J., 2015. Relation between stability and resilience determines the performance of early warning signals under different environmental drivers. *Proc. Natl. Acad. Sci.* 112 (32), 10056–10061. <https://doi.org/10.1073/pnas.1418415112>.
- de Dios, V.R., Weltzin, J.F., Sun, W., Huxman, T.E., Williams, D.G., 2014. Transitions from grassland to savanna under drought through passive facilitation by grasses. *J. Veg. Sci.* 25, 937–946. <https://doi.org/10.1111/jvs.12164>.
- De Keersmaecker, W., van Rooijen, N., Lhermitte, S., Tits, L., Schaminée, J., Coppin, P., Honnay, O., Somers, B., 2016. Species-rich semi-natural grasslands have a higher resistance but a lower resilience than intensively managed agricultural grasslands in response to climate anomalies. *J. Appl. Ecol.* 53, 430–53439. <https://doi.org/10.1111/1365-2664.12595>.
- De Vries, F.T., Liiri, M.E., Björnlund, L., Bowker, M.A., Christensen, S., Setälä, H.M., Bardgett, R.D., 2012. Land use alters the resistance and resilience of soil food webs to drought. *Nat. Clim. Chang.* 2 (4), 276.
- Deléglise, C., Meisser, M., Mosimann, E., Spiegelberger, T., Signarbieux, C., Jeangros, B., Buttler, A., 2015. Drought-induced shifts in plants traits, yields and nutritive value under realistic grazing and mowing managements in a mountain grassland. *Agric. Ecosyst. Environ.* 213, 94–104.
- Department of Science, Information Technology and Innovation (DSITI), 2017. Land Use Mapping - 1999 to Current – Queensland, State of Queensland. Accessed 2 August 2016. <http://qldspatial.information.qld.gov.au/catalogue>.
- Do, N., Kang, S., 2014. Assessing drought vulnerability using soil moisture-based water use efficiency measurements obtained from multi-sensor satellite data in Northeast Asia dryland regions. *J. Arid Environ.* 105, 22–32.
- Donohue, I., Hillebrand, H., Montoya, J.M., Petchey, O.L., Pimm, S.L., Fowler, M.S., Healy, K., Jackson, A.L., Lurgi, M., McClean, D., O'Connor, N.E., 2016. Navigating the complexity of ecological stability. *Ecol. Lett.* 19, 1172–191185. <https://doi.org/10.1111/ele.12648>.
- Dormann, C.F., Elith, J., Bacher, S., Buchmann, C., Carl, G., Carré, G., Marquéz, J.R.G., Gruber, B., Lafourcade, B., Leitão, P.J., Münckmüller, T., 2013. Collinearity: a review of methods to deal with it and a simulation study evaluating their performance. *Ecography* 36, 27–46.
- Eckert, S., Hüslér, F., Liniger, H., Hodel, E., 2015. Trend analysis of MODIS NDVI time series for detecting land degradation and regeneration in Mongolia. *J. Arid Environ.* 113, 16–11328. <https://doi.org/10.1016/j.jaridenv.2014.09.001>.
- Elith, J., Graham, C.H., Anderson, R.P., Dudík, M., Ferrier, S., Guisan, A., Hijmans, R.J., Huettmann, F., Leathwick, J.R., Lehmann, A., Li, J., Lohmann, L.G., Loiselle, B.A., Manion, G., Moritz, C., Nakamura, M., Nakazawa, Y., Overton, J.M.M., Townsend Peterson, A., Phillips, S.J., Richardson, K., Scachetti-Pereira, R., Schapire, R.E., Soberón, J., Williams, S., Wisz, M.S., Zimmermann, N.E., 2006. Novel methods improve prediction of species' distributions from occurrence data. *Ecography* 29, 129–151.
- Elith, J., Leathwick, J.R., Hastie, T., 2008. A working guide to boosted regression trees. *J. Anim. Ecol.* 77, 802–813.
- Gazol, A., Camarero, J.J., Anderegg, W.R.L., Vicente-Serrano, S.M., 2017. Impacts of droughts on the growth resilience of Northern Hemisphere forests. *Glob. Ecol. Biogeogr.* 26, 166–26176. <https://doi.org/10.1111/geb.12526>.
- Godfree, R., Lepshi, B., Reside, A., Bolger, T., Robertson, B., Marshall, D., Carnegie, M., 2011. Multiscale topographic heterogeneity increases resilience and resistance of a dominant grassland species to extreme drought and climate change. *Glob. Change Biol.* 17, 943–958.
- Grime, J.P., Fridley, J.D., Askew, A.P., Thompson, K., Hodgson, J.G., Bennett, C.R., 2008. Long-term resistance to simulated climate change in an infertile grassland. *Proceedings of the National Academy of Sciences* 105, 10028–10032. <https://doi.org/10.1073/pnas.0711567105>.
- Gu, Y., Brown, J.F., Verdin, J.P., Wardlow, B., 2007. A five-year analysis of MODIS NDVI and NDWI for grassland drought assessment over the central Great Plains of the United States. *Geophys. Res. Lett.* 34, L06407. <https://doi.org/10.1029/2006GL029127>.
- Hafeez, M., Frost, A.J., Vaze, J., Smith, A., Elmahdi, A., 2015. A New integrated continental hydrological simulation system: an overview of the Australian Resource Assessment Modelling System (AWRAMS). *Water: J. Aust. Water Assoc.* v42, 75–82.
- Hall, T.J., Jones, P., Silcock, R.G., Filet, P.G., 2016. Pasture production and composition response after killing Eucalypt trees with herbicides in central Queensland. *Rangel. J.* 38, 427–441. <https://doi.org/10.1071/RJ16013>.
- Hastie, T., Tibshirani, R., Friedman, J.H., 2001. *The Elements of Statistical Learning: Data Mining, Inference, and Prediction*. Springer-Verlag, New York.
- Hofer, D., Suter, M., Haughey, E., Finn, J.A., Hoekstra, N.J., Buchmann, N., Lüscher, A., 2016. Yield of temperate forage grassland species is either largely resistant or resilient to experimental summer drought. *J. Appl. Ecol.* 53, 1023–1034. <https://doi.org/10.1111/1365-2664.12694>.
- Hoover, D.L., Knapp, A.K., Smith, M.D., 2014. Resistance and resilience of a grassland ecosystem to climate extremes. *Ecology* 95, 2646–2656. <https://doi.org/10.1890/13-2186.1>.
- Hua, T., Wang, X., Zhang, C., Lang, L., Li, H., 2017. Responses of vegetation activity to drought in Northern China. *Land Degrad. Dev.* 28, 1913–281921. <https://doi.org/10.1002/ldr.2709>.
- Huete, A., Didan, K., Miura, T., Rodriguez, E.P., Gao, X., Ferreira, L.G., 2002. Overview of the radiometric and biophysical performance of the MODIS vegetation indices. *Remote Sens. Environ.* 83, 195–213.
- Hundecha, Y., Bárdossy, A., 2005. Trends in daily precipitation and temperature extremes across western Germany in the second half of the 20th century. *Int. J. Climatol.* 25, 1189–251202. <https://doi.org/10.1002/joc.1182>.
- Kath, J., Powell, S., Reardon-Smith, K., El Sawah, S., Jakeman, A.J., Croke, B.F.W., Dyer, F.J., 2015. Groundwater salinization intensifies drought impacts in forests and reduces refuge capacity. *J. Appl. Ecol.* 52, 1116–521125. <https://doi.org/10.1111/1365-2664.12495>.
- Kawamura, K., Akiyama, T., Yokota, H.O., Tsutsumi, M., Yasuda, T., Watanabe, O., Wang, S., 2005. Quantifying grazing intensities using geographic information systems and satellite remote sensing in the Xilingol steppe region, Inner Mongolia. *China. Agric. Ecosyst. Environ.* 107, 83–93.
- Kendall, M., 1955. *Rank Correlations Methods*, 2nd ed. Griffin, London.
- Le Brocq, A.F., Kath, J., Reardon-Smith, K., 2018. Chronic groundwater decline: a multi-decadal analysis of groundwater trends under extreme climate cycles. *J. Hydrol.* 561, 976–561986. <https://doi.org/10.1016/j.jhydrol.2018.04.059>.
- Lindborg, R., Bengtsson, J., Berg, Å., Cousins, S.A., Eriksson, O., Gustafsson, T., Hasund, K.P., Lenoir, L., Pihlgren, A., Sjödin, E., Stenseke, M., 2008. A landscape perspective on conservation of semi-natural grasslands. *Agric. Ecosyst. Environ.* 125, 213–222.
- Luo, W., Wang, X., Sardans, J., Wang, Z., Dijkstra, F.A., Lü, X.-T., Peñuelas, J., Han, X., 2018. Higher capability of C3 than C4 plants to use nitrogen inferred from nitrogen stable isotopes along an aridity gradient. *Plant Soil* 428, 93–103. <https://doi.org/10.1007/s11104-018-3661-2>.
- Lymburner, L., Tan, P., Mueller, N., Thackway, R., Lewis, A., Thankappan, M., Randall, L., Islam, A., Senarath, U., 2011. *The National Dynamic Land Cover Dataset*, Geoscience Australia, Symonston, ACT, Australia. Record 2011/31. pp. 95 ISBN 978-1-921954-30-6.
- McLeod, A.I., 2011. Kendall: Kendall Rank Correlation and Mann-kendall Trend Test. R Package Version 2.2. <http://CRAN.R-project.org/package=Kendall>.
- Menzel, A., Fabian, P., 1999. Growing season extended in Europe. *Nature* 397 659–659.
- Moreno, G., 2008. Response of understorey forage to multiple tree effects in Iberian dehesas. *Agric. Ecosyst. Environ.* 123, 239–244.
- Neuwirth, C., Hofer, B., 2013. Spatial sensitivity of grassland yields to weather variations in Austria and its implications for the future. *Appl. Geogr.* 45, 332–341.
- Nimmo, D.G., Mac Nally, R., Cunningham, S.C., Haslem, A., Bennett, A.F., 2015. Vive la résistance: reviving resistance for 21st century conservation. *Trends Ecol. Evol.* (Amst.) 30, 516–523. <https://doi.org/10.1016/j.tree.2015.07.008>.
- Oliver, T.H., Morecroft, M.D., 2014. Interactions between climate change and land use change on biodiversity: attribution problems, risks, and opportunities. *WIREs Clim. Change* 5, 317–5335. <https://doi.org/10.1002/wcc.271>.
- Otkin, J.A., Anderson, M.C., Hain, C., Svoboda, M., Johnson, D., Mueller, R., Tadesse, T., Wardlow, B., Brown, J., 2016. Assessing the evolution of soil moisture and vegetation conditions during the 2012 United States flash drought. *Agric. For. Meteorol.* 218, 230–218242. <https://doi.org/10.1016/j.agrformet.2015.12.065>.
- Parviainen, M., Luoto, M., Heikkinen, R.K., 2009. The role of local and landscape level measures of greenness in modelling boreal plant species richness. *Ecol. Modell.* 220, 2690–2701.
- Pearson, R.K., 1999. Data cleaning for dynamic modeling and control. *European Control Conference*.
- Pettorelli, N., Vik, J.O., Mysterud, A., Gaillard, J.M., Tucker, C.J., Stenseth, N.C., 2005. Using the satellite-derived NDVI to assess ecological responses to environmental change. *Trends Ecol. Evol.* 20, 503–510.
- Polley, H.W., Briske, D.D., Morgan, J.A., Wolter, K., Bailey, D.W., Brown, J.R., 2013. Climate change and North American rangelands: trends, projections, and implications. *Rangel. Ecol. Manage.* 66, 493–511. <https://doi.org/10.2111/REM-D-12-00068.1>.
- R Core Team, 2016. R: a Language and Environment for Statistical Computing. R Foundation for Statistical Computing, Vienna, Austria. <http://www.R-project.org/>.
- Ridgeway, G., 2012. Gbm: Generalized Boosted Regression Models. R Package Version 1.6-3.2. Available at: Accessed 27.08.2016. <http://cran.r-project.org/web/packages/gbm/index.html>.
- Robinson, T.P., Wint, G.W., Conchedda, G., Van Boeckel, T.P., Ercoli, V., Palamara, E., Cinardi, G., D'Aiuti, L., Hay, S.I., Gilbert, M., 2014. Mapping the global distribution of livestock. *PLoS One* 9 (5), e96084.
- Smith, M.D., 2011. An ecological perspective on extreme climatic events: a synthetic definition and framework to guide future research. *J. Ecol.* 99, 656–663. <https://doi.org/10.1111/j.1365-2745.2011.01798.x>.
- TERN AusCover, 2016a. Enhanced Vegetation Indices 16-Day 250m - Terra/MOD13Q1. obtained from: made available by the AusCover facility (<http://www.auscover.org.au>) of the Terrestrial Ecosystem Research Network (TERN, <http://www.tern.org.au>). (Accessed 20 July 2016). <http://data.auscover.org.au/thredds/auscover/lpdaac-aggregates/c5/v2-nC4/auscover/MOD13Q1.005/catalog.html>.
- TERN AusCover, 2016b. MODIS Gross Primary Productivity - DIFFUSE Algorithm With Three-Veg-Type Parameterisation, Retrieved From the Online Data Pool, Courtesy of the NASA Land Processes Distributed Active Archive Center (LP DAAC), USGS/Earth Resources Observation and Science (EROS) Center, Sioux Falls, South Dakota. and made available by the AusCover facility (<http://www.auscover.org.au>) of the Terrestrial Ecosystem Research Network (TERN, <http://www.tern.org.au>). (Accessed 04 March 2017). https://lpdaac.usgs.gov/data/access/data_pool.

- Trenberth, K.E., Dai, A., van der Schrier, G., Jones, P.D., Barichivich, J., Briffa, K.R., Sheffield, J., 2013. Global warming and changes in drought. *Nat. Clim. Chang.* 4, 17–422. <https://doi.org/10.1038/nclimate2067>.
- Tubiello, F.N., Soussana, J.F., Howden, S.M., 2007. Crop and pasture response to climate change. *Proc. Natl. Acad. Sci.* 104, 19686–19690.
- Viney, N., Vaze, J., Crosbie, R., Wang, B., Dawes, W., Frost, A., 2015. AWRA-L v5.0: Technical Description of Model Algorithms and Inputs. CSIRO, Australia.
- Zhang, X., Vincent, L.A., Hogg, W.D., Niitsoo, A., 2000. Temperature and precipitation trends in Canada during the 20th century. *Atmos.-Ocean* 38, 395–429.